Inorganic Chemistry

Article

pubs.acs.org/IC

Rational Organization of Lanthanide-Based SMM Dimers into Three-Dimensional Networks

Xiaohui Yi, Guillaume Calvez, Carole Daiguebonne, Olivier Guillou, and Kevin Bernot*

INSA, ISCR, UMR 6226, Université Européenne de Bretagne, 35708 Rennes, France

Supporting Information

ABSTRACT: Optimization of the reaction of $[Ln(hfac)_3]\cdot 2H_2O$ and pyridine-N-oxide (PyNO), which is known to afford double-bridged dimers, leads to triple-bridged dimers of formula $[(Ln(hfac)_3)_2(PyNO)_3]$ (Ln = Gd (**1**), Dy (**2**)) from which the Dy derivative (**2**) behaves as a single-molecule magnet (SMM). The pseudo threefold axis symmetry of this zero-dimensional building block makes possible its extension into a tridimensional network. By changing PyNO for 4,4′-bipyridine *N*,*N*′-dioxide (4,4′BipyNO) a tridimensional compound of formula $\{[Ln(hfac)_3]_2(4,4'BipyNO)_2]\}$ (Ln = Eu (**3**), Gd (**4**), and Dy (**5**)) is then rationally obtained. This covalent three-dimensional (3D) network has a remarkably high cell volume (V = 24 419 A^3) and is an arrangement of interpenetrated 3D subnetworks whose triple-bridged dimers still behave as SMMs.

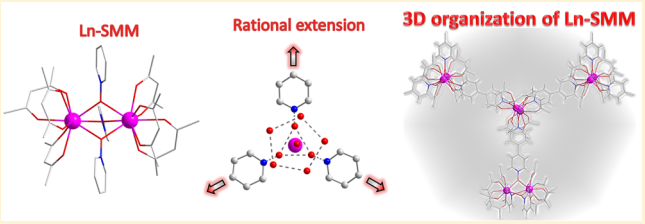

INTRODUCTION

Rational organization of pre-existing molecular building blocks is a fundamental tool in coordination chemistry.[1,2] This strategy allows obtaining either original compounds of fundamental interest or high-performance materials for targeted applications.[3−9] Molecular magnetism is a research area in which this technique has been widely used especially as soon as high-temperature molecular magnets were targeted.[10,11] This technique also permitted the association of different magnetic centers into extended structure through step-by-step synthesis and to a better control of the overall magnetic behavior.[12−14] It is also at the origin of the design of one-dimensional compounds such as molecular chains.[15−21] In all these previous cases the linkers and the ways they are connected to the magnetic node are fundamental as they had to transmit as much magnetic interaction as possible between the magnetic ions.[22]

On another hand, magnetism of discrete molecules has developed quickly as new original physical properties emerged.[23−26] Organization of magnetic ions into discrete entities (zero-dimensional) has allowed the observation of magnetic properties at the molecular level and opened the field of single-molecule magnets (SMMs).[27,28] These molecules have shown remarkable magnetic properties but also significant phenomena such as quantum tunneling of the magnetization[29,30] or Berry phase interference effect.[31] They are also expected to be good candidates for spintronics applications[32−35] or surface-based devices.[36]

It is then exciting to organize SMM into wider molecular edifices[37−39] to combine their local magnetic properties with those of extended molecular architectures such as coordination polymers or metal−organic frameworks.[40,41] Such coordination networks with magnetic properties based on SMM behavior have been reviewed recently,[11] but few of them are actually purely three-dimensional[39,42] (3D) and even fewer with lanthanide-based SMMs.[43,44] Lanthanide ions have boosted the design of SMMs during the past decade[45] as their magnetic anisotropy[46,47] offer new perspectives on magnetic relaxation properties.[48−54] However, their sensibility to their chemical environment[48,55−60] is a drawback. In fact, if lanthanide ions with poorly rigid first coordination sphere are considered, their SMM properties may vanish upon 3D organization as deformation toward low-symmetry environment occurs. A possibility is to work with hydrogen-rich ligands and rely on hydrogen bonding to create a 3D network,[61] but this is a highly serendipitous strategy.

In this work we choose to use rigid lanthanide SMM dimers and to modify them to allow their organization into 3D network. We recently reported a detailed investigation on lanthanide-based dimers of formula $[Ln(hfac)_3PyNO]_2$ (hfac = hexafluoro-acetylacetonate, PyNO = 4-pyridine-N-oxide).[62] These dimers show very good SMM behavior (Δ = 167 K for Dy derivative) together with nice evaporability and luminescence properties. However, organization of these dimers into an extended network is difficult because the two bridging ligands that could allow further connection are at 180° one from the other, and only two-dimensional networks can be rationally targeted.

We overcome this drawback by designing three-bridged dimers of formula $[Ln(hfac)_3]_2(PyNO)_3]$ (Ln = Gd (**1**), Dy (**2**)) that also behave as SMMs. The bridging ligands point at 120° from the center of the dimers and allow the rational design of 3D network of SMM of formula $\{[Ln(hfac)_3]_2$-$(4,4'BipyNO)_3\}_\infty$ (Ln = Eu (**3**), Gd (**4**), Dy (**5**), and

Received: January 12, 2015
Published: May 13, 2015

DOI: 10.1021/acs.inorgchem.5b00087
Inorg. Chem. 2015, 54, 5213−5219

4,4′BipyNO = 4,4′-bipyridine *N*,*N*′-dioxide). To the best of our knowledge this is the first rationally designed covalent 3D network made of Ln-based SMMs.

EXPERIMENTAL SECTION

Starting Materials. All reagents were of analytical grade and used as received. $[Ln(hfac)_3]\cdot 2H_2O$ precursors were synthesized accordingly to previously reported methods.[62] PyNO and 4,4′BipyNO were purchased from TCI chemicals.

Synthesis of the Crystal and Powders of $[Ln(hfac)_3]_2(PyNO)_3$ (Ln = Gd (1), Dy (2)). $Ln(hfac)_3(H_2O)_2$ (0.2 mmol) is dissolved in 15 mL of boiling *n*-heptane. Then a 10 mL dry $CHCl_3$ solution of PyNO (0.4 mmol) is added. The resulting boiling mixture is stirred for 5 min, then cooled to room temperature. After some days of slow evaporation, big colorless prisms are obtained. Powders are obtained by grinding the crystals. Anal. Calcd (%) for powder of **1**: C_{45} H_{21} F_{36} O_{15} N_3 Gd_2 C 29,30, H 1,14, N 2,28; found: C 29.12, H 1.18, N 2.20.

Synthesis of the Crystal of Compound $\{[Eu(hfac)_3]_2(4,4'BipyNO)_3\}_\infty$ (3). $Eu(hfac)_3(H_2O)_2$ (0.05 mmol) is added to 5 mL of $CHCl_3$. This solution is then covered by a 3 mL 4,4′BiPyNO (0.05 mmol) CH_3OH solution. The resulting two-layered solution is sealed and kept at room temperature. The crystals suited for single-crystal X-ray diffraction are obtained after several days.

Synthesis of the Powders of Compound $\{[Ln(hfac)_3]_2(4,4'BipyNO)_3\}_\infty$ (Ln = Gd (4), Dy (5)). $Ln(hfac)_3(H_2O)_2$ (0.1 mmol) is added to 15 mL of $CHCl_3$. Then a 20 mL dry cool $CHCl_3$ solution of 4,4′BipyNO (0.2 mmol) is added. A precipitate appears and is filtered. Anal. Calcd (%) for powders of **4** and **5**: C_{45} H_{18} F_{36} O_{15} N_3 Gd_2 C 29.35, H 0.98, N 2.28; found C 29.01, H 1.25, N 2.10. C_{45} H_{18} F_{36} O_{15} N_3 Dy_2 C 29.16, H 0.98, N 2.27; found C 28.97, H 1.28, N 2.18.

RESULTS AND DISCUSSION

Structure Description. Compound **2** of formula $[Dy(hfac)_3]_2(PyNO)_3]$ crystallizes in the $P2_1/c$ space group (No. 14). The main structural data are reported in Table 1, and the molecular structure is shown in Figure 1. The molecule is made of two $Dy(hfac)_3$ moieties connected by three PyNO molecules. Two crystallographically independent Dy^{III} ions are found. The oxygen atoms (O1, O2, and O3) of three PyNO ligands link these two Dy^{III} ions in μ_2 mode. Both Dy^{III} ions are nine-coordinated by six oxygen atoms from $hfac^-$ ligands and three oxygen atoms from PyNO. The $Dy-O_{hfac}$ bond lengths are in the range of 2.34(1)−2.42(8) Å. The $Dy-O_{PyNO}$ bonds are longer with a bond length range of 2.42(8)−2.44(9) Å. Selected bonds distance and angles are listed in Supporting Information, Table S1. According to the calculation results of SHAPE software,[63−65] both Dy ions are in a distorted capped square antiprism coordination environment of C_{4v} symmetry (Supporting Information, Figure S1 and Table S2). The square planes of the antiprism for Dy1 are formed by O1, O3, O4, O5 and O2, O6, O7 O8, for Dy2, by O2, O1, O13, O12 and O14 O15, O10, O3, respectively. The capped square antiprism geometry of Dy1 is more distorted than the one of Dy2 (C_{4v} SHAPE factor for Dy1 is 0.927 and SHAPE factor for Dy2 is 0.605). The intramolecular Dy−Dy distance is 3.86(1) Å. Each dimer is well-isolated, and the shortest interdimer Dy−Dy distance is 9.912(4) Å (Figure 1). Isostructurality of **1** with **2** is confirmed on the basis of comparison of X-ray diffraction powder patterns (Supporting Information, Figure S2).

In compounds **1** and **2** the three bridging PyNO ligands point at 120° from the middle of the dimer (Figure 2). Consequently the substitution of PyNO ligand for the bis-monodentate 4,4′BipyNO can make possible the organization of the dimers into an extended network. Two phases slow diffusion of Eu-based precursor and 4,4′BipyNO affords single crystals of $\{[Eu(hfac)_3]_2(4,4'BipyNO)_3\}_\infty$ (**3**). Despite great synthetic efforts the Eu^{III} derivative is the only one that has been obtained as single crystal, but the isostructurality of the other derivatives that contain Gd (**4**) or Dy(**5**) are evidenced on the basis of comparison of X-ray powder patterns (Supporting Information, Figure S4).

Compound **3** crystallizes in the *F*2*dd* space group (No. 43) with an asymmetric unit composed of two $Eu(hfac)_3$ motifs and two 4,4′BipyNO ligands. Each $Eu(hfac)_3$ motif is connected to three 4,4BipyNO ligands that point at 120° from the middle of the dimer and form a 3D coordination framework that crystallize with a quite high cell volume (24 420 $Å^3$; Figure 2). This validates the rational design approach previously described.

Main structural parameters are listed in Table 1. Two crystallographically independent Eu^{III} centers are found in the asymmetric unit (Figure 2). Both Eu ions are nine-coordinated and surrounded by six oxygen atoms from $hfac^-$ ligands and three oxygen atoms from 4,4′BipyNO N-oxide groups. The bond lengths around Eu1 and Eu2 are similar. ($Eu1-O_{hfac-}$ = 2.34(7)−2.44(7) Å, $Eu1-O_{4,4'BipyNO}$ = 2.16(0)−2.51(8) Å, $Eu2-O_{hfac-}$ = 2.37(9)−2.43(7), and $Eu2-O_{N\text{-}Oxide}$ = 2.44(8)−2.54(7) Å). Selected bond data are listed in Supporting Information, Table S3. Both Eu ions are in a distorted capped square antiprism coordination environments (C_{4v})[63−65] (Supporting Information, Figure S3). Intradimer distances are 3.94(1) and 3.93(2) Å for Eu1−Eu1 and Eu2−Eu2, respectively. Each dimer is well-isolated, with the shortest interdimer Eu−Eu distance of 12.04(7) Å.

The topological analysis of **3** by TOPOS software[66] reveals that the obtained 3D network belongs to the $ThSi_2$ network family (Figure 3). If the Eu^{III} dimers are considered as three-connected nodes and 4′4BipyNO as linkers, then each node has three angles, and each of the angles is part of a 10-membered shortest circuit. Consequently the 3D network has the Wells point symbol (10,3)-b. Each single 3D network consists of large windows (40 × 12.55 Å) that are filled via mutual

Table 1. Table of Main Crystallographic Parameters of 2 and 5

complex	**2**	**5**
formula	$C_{45}H_{21}F_{36}O_{15}N_3Dy_2$	$C_{45}H_{18}F_{36}O_{15}N_3Eu_2$
M [g mol^{-1}]	1852.62	1828.57
crystal system	monoclinic	orthorhombic
space group	$P2_1/c$ (No. 14)	*F*2*dd* (No. 43)
a [Å]	19.573(3)	23.59(5)
b [Å]	14.570(5)	28.12(5)
c [Å]	21.236(5)	36.80(5)
α [deg]	90.00	90
β [deg]	92.948	90
γ [deg]	90.00	90
V [Å^3]	6048(3)	24 419
Z	4	16
T [K]	150(2)	150(2)
2θ range	2.03−27.45	2.03−27.45
reflns collected	13 765	32 925
independent reflns	10 584	13 453
observed reflns	5010	10 909
parameters	910	913
$R1/\omega R^2$	0.051/0.051/0.1707	0.057/0.1706
GOF	0.988	1.073

DOI: 10.1021/acs.inorgchem.5b00087
Inorg. Chem. 2015, 54, 5213−5219

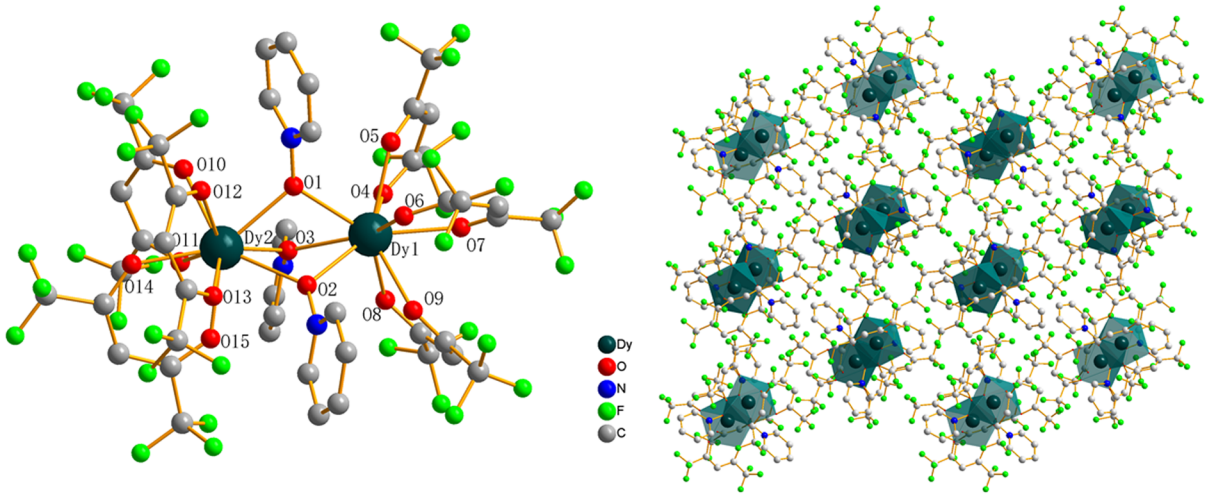

Figure 1. (left) Representation of the $[(Dy(hfac)_3)_2(PyNO)_3]$ (**2**) dimer with labeling scheme. (right) Projection view of the crystal packing of $[(Dy(hfac)_3)_2(PyNO)_3]$ (**2**) along the *b* axis. Hydrogen atoms omitted for clarity.

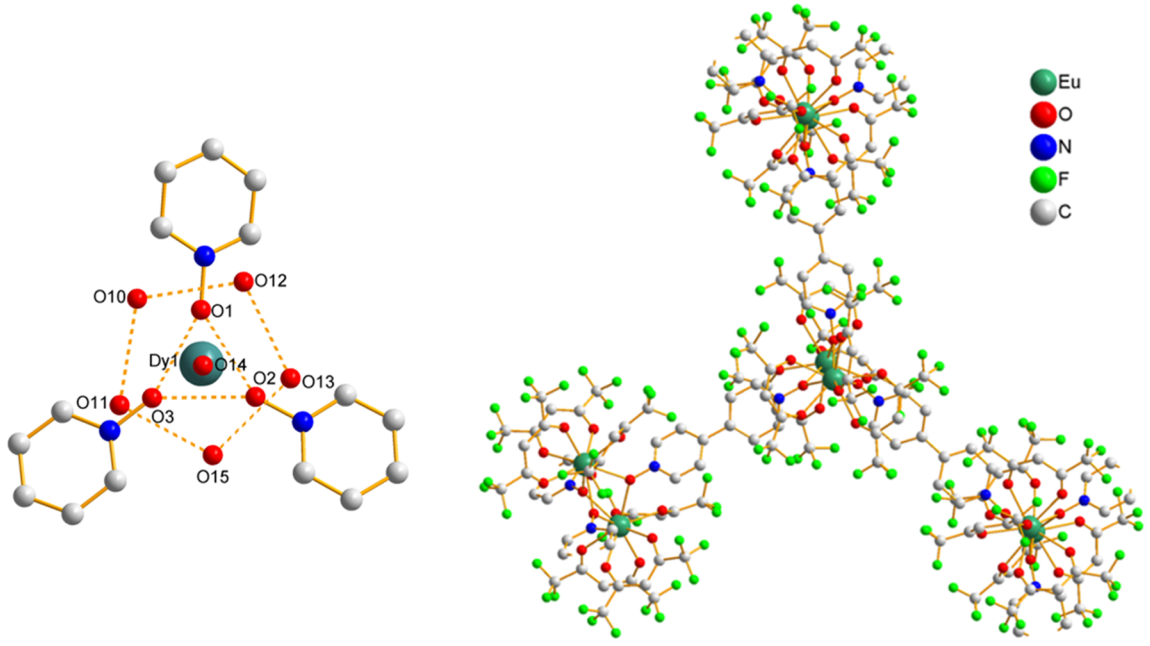

Figure 2. (left) Representation of the $[(Dy(hfac)_3)_2(PyNO)_3]$ (**2**) dimer core with the three PyNO ligands pointing at 120° from each other. (right) Representation of $\{[Eu(hfac)_3]_2(BipyNO)_3\}_\infty$ (**3**) with the three-connected $[Eu(hfac)_3]_2$ dimers. Hydrogen atoms omitted for clarity.

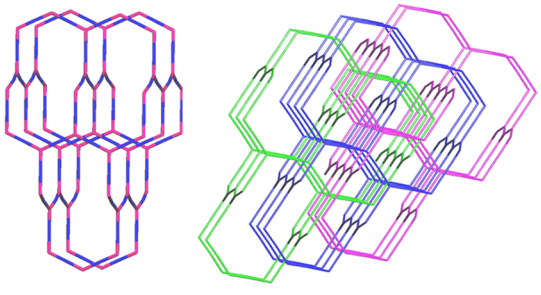

Figure 3. Topological representation of the threefold network of **3**. (left) Simplified single $ThSi_2$ network, red three-connected point are Eu-based dimers, blue stick are 4,4′BipyNO ligands. (right) Overall representation of the interpenetrated networks.

interpenetration of three independent equivalent networks, generating a threefold interpenetrated 3D network (Figure 3).

Magnetic Properties. To have some insight into the Ln^{III}–Ln^{III} interaction in the dimers $\chi_M T$ versus T curves of the Gd derivatives of the dimer (**1**) and the 3D network (**4**) were measured (Supporting Information, Figures S5 and S6). On both compounds weak antiferromagnetic coupling is observed (see Supporting Information). The direct current (dc) magnetic properties of the corresponding Dy^{III}-based compounds **2** and **5** were investigated under a 1000 Oe field in the temperature range of 1.8−300 K (Figure 4). At room temperature, the $\chi_M T$ values of both compounds are 27.17 and 27.72 emu K mol^{-1}, respectively. These values are in good agreement with the expected theoretical values (28.34 emu K mol^{-1}) for two noninteracting Dy ions ($^6H_{15/2}$, $S = 5/2$, $L = 5$, g

DOI: 10.1021/acs.inorgchem.5b00087
Inorg. Chem. 2015, 54, 5213−5219

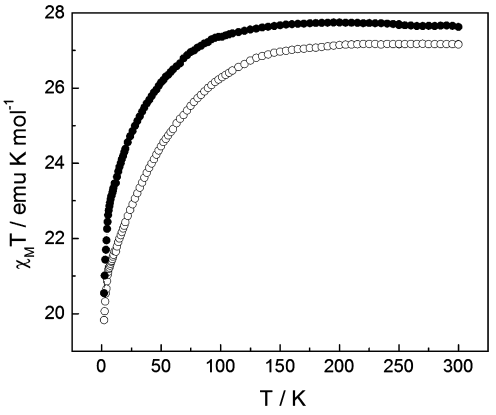

Figure 4. Temperature dependence of $\chi_M T$ for **2** (○) and **5** (●).

= 4/3). When the compounds cooled, the $\chi_M T$ values of both compounds decrease because of a progressive depopulation of the levels of the J = 15/2 multiplet of the Dy^{III} ions.

This phenomenon hampers the direct determination of the nature of the magnetic exchange interaction in the dimer. Common estimation of Dy−Dy interaction can be provided by considering Stevens crystal-field parameters of a given geometry around the lanthanide to reproduce $\chi_M T$ versus T curves. In our case this procedure was not possible for two main reasons: (i) strong distortion from ideal symmetry of the coordination polyhedra are observed and (ii) two crystallographically independent Ln^{III} must be considered, which leads to system overparametrizaton.

To characterize the SMM properties of compounds **2** and **5**, the in-phase χ_M' and the out-of-phase χ_M'' components of the alternating current (ac) susceptibility were measured at various frequencies with a 3 Oe oscillating field. Compound **2** exhibits out-of-phase signal in zero dc field that is found temperature-independent possibly because of the occurrence of a fast relaxation of the magnetization (≃800 Hz) through a quantum tunneling mechanism. At that stage in-field ac measurements can be performed to suppress this fast relaxation mechanism. For compound **2**, the dc field that induces the slowest relaxation is H_{dc} = 1900 Oe (Figure 5). Clear frequency dependence of the in-phase and out-of-phase components of χ_M' and χ_M'' (Figure 6 and Supporting Information, Figure S7) is then observed. However, a double relaxation process is visible at low temperature[67] (2−4 K region), probably because each Dy contributes to χ_M'' in a different temperature range. On **5**, this overall picture is shifted toward high frequency so as the zero field relaxation is not visible anymore and H_{dc} = 1900 Oe induces a magnetic relaxation that is 30 times faster (Figures 5, 6, and Supporting Information, Figure S8).

The χ_M'' versus frequency curves of both compounds were fitted by an extended Debye model, and the extracted relaxation times are reported in Figure 7 and Supporting Information, Tables S5 and S6. For compound **2**, the shoulder observed in the χ_M'' versus T plot induces a bumpy Arrhenius plot at low temperature. However, at high temperature, the relaxation is governed by a thermally activated mechanism. The fitting of the Arrhenius plot gives an effective energy barrier of 24.4 K and a $\tau_0 = 3.18 \times 10^{-6}$ s. For compound **5**, the fitting of the Arrhenius plot gives a lower effective energy barrier of 10.3 K and a $\tau_0 = 1.25 \times 10^{-5}$ s. These τ_0 values are likely to highlight additional relaxation processes in the compounds.[67]

It is worth noticing that two other examples of 3D arrays of Ln-based SMMs have been reported.[43,44] They both rely on association of carboxylate-based ligand and lanthanides under hydrothermal conditions. Depending on the arrays, the magnetic properties are very significant[43] or rather poor,[44] illustrating the serendipity of this approach. Moreover this one-step synthesis does not allow for independent study of the magnetic building blocks of the compounds.

Our group has previously reported a dimer that is similar to **1** and **2** but where the two $Dy(hfac)_3$ moieties are bridged by two and not three pyridine-N-oxide ligands.[62] The Dy^{III} ion is then eight-coordinated in a D_{4d} site symmetry (square antiprism), and the compound shows remarkable SMM properties (Δ = 167 K). Obviously, the O9 coordination of the Dy^{III} in **2** and **5** is less favorable to an equatorial stabilization of the 4f electron density ("oblate" ion)[48] and to enhance a SMM behavior. However, this O9 geometry is an asset as soon as one wants to organize the dimers into tridimensional molecular architectures.

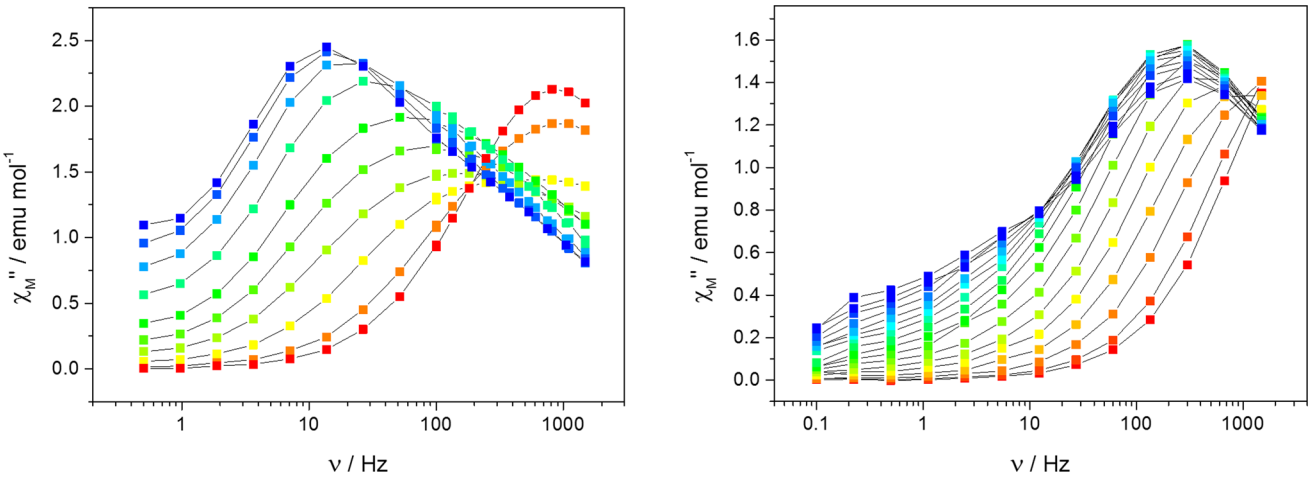

Figure 5. (left) Field dependence of the *out-of*-phase component of the magnetization of **2** at 2 K. Color mapping from 0 (red) to 2200 Oe (blue). (right) Field dependence of the *out-of*-phase component of the magnetization of **5** at 2.5 K. Color mapping from 0 (red) to 2800 Oe (blue). Lines are guides to the eye.

DOI: 10.1021/acs.inorgchem.5b00087
Inorg. Chem. 2015, 54, 5213−5219

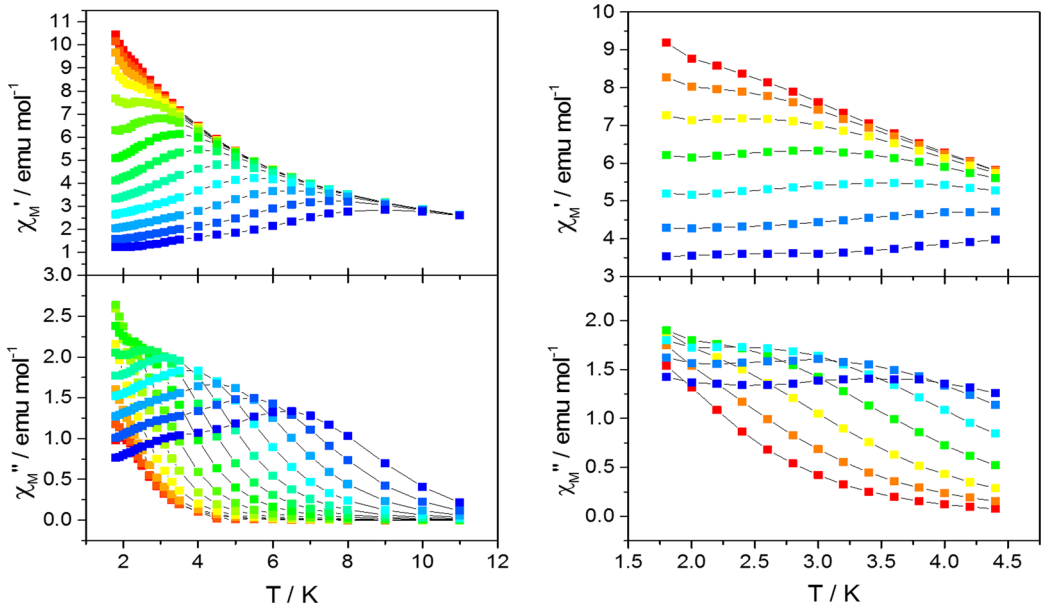

Figure 6. Temperature dependence of the *in*-phase susceptibility (upper left) and the *out-of*-phase susceptibility (lower left) with H_{dc} = 1900 Oe for **2** with color mapping from 0.5 Hz (red) to 1500 Hz (blue). Temperature dependence of the *in*-phase susceptibility (upper right) and the *out-of*-phase susceptibility (lower right) with H_{dc} = 1900 Oe for **5** with color mapping from 14 Hz (red) to 1500 Hz (blue).

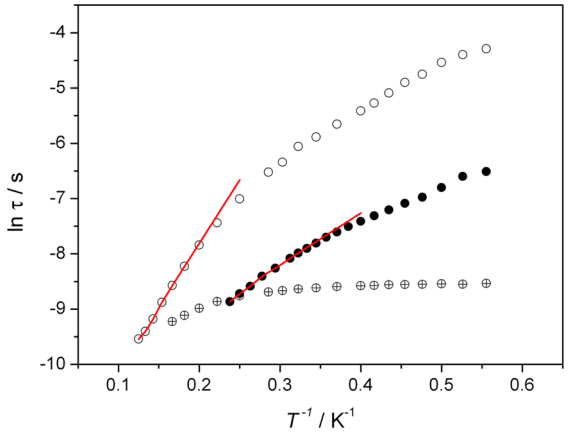

Figure 7. Relaxation time (τ) plotted against T^{-1} with the best linear fit of the high-temperature region for **2** with H_{dc}= 0 (⊕) and 1900 Oe (○) and **5** (●) H_{dc} = 1900 Oe.

CONCLUSION

In this paper, we present a three-bridged dimer $[(Ln(hfac)_3)_2(PyNO)_3]$ (Ln = Gd (**1**), Dy (**2**)) generated by the reaction of $Ln(hfac)_3(H_2O)_2$ and PyNO. Compound **2** is an in-field SMM. The structural peculiarity of this zero-dimensional dimer allows its extension into an infinite coordination network by changing its bridging ligand for a bis-bridging one. The 3D compound $\{[Ln(hfac)_3]_2(4,4'BipyNO)_3\}_\infty$ (Ln = Eu (**3**), Gd (**4**), Dy (**5**)) is a triple-interpenetrated open framework with TiSh2 topology with triply interconnected lanthanide dimers. In **5**, SMM behavior of the dimers is still visible validating this rational approach. This is a step forward in the search for 3D frameworks based on SMMs. Further optimization of this network may be achieved by using more rigid and/or bulkier ligands than 4,4′BipyNO to avoid distortion of the lanthanide environment and interpenetration of the network. This may optimize the SMM properties and provide porosity to the compound. Such metal organic framework based on Dy-SMMs would offer nice perspective as soon as interplay between MOF properties[68,69] and SMMs are targeted[70] as, for example, guest-tuning of SMMs and/or of luminescent properties.

ASSOCIATED CONTENT

Supporting Information

Selected bond angles and distances, illustrated coordination environments, SHAPE factor data, X-ray powder diffraction patterns, plots indicating temperature dependence of $\chi_M T$ and frequency dependence of in-phase and out-of-phase components of magnetization, data extracted from plots, explanation of fitting procedure, crystallographic data in CIF files. The Supporting Information is available free of charge on the ACS Publications website at DOI: 10.1021/acs.inorgchem.5b00087.

AUTHOR INFORMATION

Corresponding Author

*E-mail: kevin.bernot@insa-rennes.fr.

Notes

The authors declare no competing financial interest.

ACKNOWLEDGMENTS

We acknowledge financial support from Chinese Scholarship Council (CSC) and Rennes Métropole. T. Guizouarn and G. Poneti are also acknowledged.

REFERENCES

(1) Ribas, J. *Coordination Chemistry;* Wiley-VCH: Weinheim, Germany, 2008.
(2) Verdaguer, M.; Launay, J.-P. *Electrons in Molecules; From Basic Principles to Molecular Electronics;* Oxford University Press: Oxford, U.K., 2013.
(3) Ferlay, S.; Mallah, T.; Ouahes, R.; Veillet, P.; Verdaguer, M. *Nature* **1995**, *378*, 701−703.
(4) Manriquez, J. M.; Yee, G. T.; Mclean, R. S.; epstein, A. J.; Miller, J. S. *Science* **1991**, *252*, 1415−1417.
(5) Entley, W. R.; Girolami, G. S. *Science* **1995**, *268*, 397−400.
(6) Ferey, G. *J. Solid State Chem.* **2000**, *152*, 37−48.

DOI: 10.1021/acs.inorgchem.5b00087
Inorg. Chem. 2015, 54, 5213−5219

(7) Dalgarno, S. J.; Power, N. P.; Atwood, J. L. *Coord. Chem. Rev.* **2008**, *252*, 825−841.
(8) Shi, X.; Zhu, G. S.; Fang, Q. R.; Wu, G.; Tian, G.; Wang, R. W.; Zhang, D. L.; Xue, M.; Qiu, S. L. *Eur. J. Inorg. Chem.* **2004**, 185−191.
(9) Busch, D. H.; Stephenson, N. A. *Coord. Chem. Rev.* **1990**, *100*, 119−154.
(10) Pedersen, K. S.; Bendix, J.; Clerac, R. *Chem. Commun.* **2014**, *50*, 4396−4415.
(11) Jeon, I. R.; Clérac, R. *Dalton Trans.* **2012**, *41*, 9569−9586.
(12) Lescouezec, R.; Vaissermann, J.; Ruiz-Perez, C.; Lloret, F.; Carrasco, R.; Julve, M.; Verdaguer, M.; Dromzee, Y.; Gatteschi, D.; Wernsdorfer, W. *Angew. Chem., Int. Ed.* **2003**, *42*, 1483−1486.
(13) Winpenny, R. E. P. *Chem. Soc. Rev.* **1998**, *27*, 447−452.
(14) Huang, Y. G.; Jiang, F. L.; Hong, M. C. *Coord. Chem. Rev.* **2009**, *253*, 2814−2834.
(15) Lecren, L.; Wernsdorfer, W.; Li, Y. G.; Vindigni, A.; Miyasaka, H.; Clerac, R. *J. Am. Chem. Soc.* **2007**, *129*, 5045−5051.
(16) Coulon, C.; Miyasaka, H.; Clérac, R. In *Single-Molecule Magnets and Related Phenomena;* Winpenny, R., Ed.; Springer: Berlin Heidelberg, 2006; Vol. *122*, pp 163−206.
(17) Coulon, C.; Clérac, R.; Lecren, L.; Wernsdorfer, W.; Miyasaka, H. *Phys. Rev. B* **2004**, *69*, 132408.
(18) Gatteschi, D.; Sessoli, R.; Caneschi, A.; Bogani, L.; Vindigni, A. Proceedings of the 225th National Meeting of the American Chemical Society, New Orleans, Louisiana; American Chemical Society: Washington, DC, 2003; pp U147−U147.
(19) Bogani, L.; Sangregorio, C.; Sessoli, R.; Gatteschi, D. *Angew. Chem., Int. Ed.* **2005**, *44*, 5817−5821.
(20) Bernot, K.; Bogani, L.; Caneschi, A.; Gatteschi, D.; Sessoli, R. *J. Am. Chem. Soc.* **2006**, *128*, 7947−7956.
(21) Bogani, L.; Vindigni, A.; Sessoli, R.; Gatteschi, D. *J. Mater. Chem.* **2008**, *18*, 4750−4758.
(22) Kahn, O. *Molecular Magnetism;* Wiley-VCH: Weinheim, Germany, 1993.
(23) Gatteschi, D.; Bogani, L. *Phys. Chem. Chem. Phys.* **2014**, *16*, 18076−18082.
(24) Meier, F.; Levy, J.; Loss, D. *Phys. Rev. Lett.* **2003**, *90*, 047901.
(25) Leuenberger, M. N.; Loss, D. *Nature* **2001**, *410*, 789−793.
(26) Miller, J. S.; Gatteschi, D. *Chem. Soc. Rev.* **2011**, *40*, 3065−3066.
(27) Gatteschi, D.; Bogani, L.; Cornia, A.; Mannini, M.; Sorace, L.; Sessoli, R. *Solid State Sci.* **2008**, *10*, 1701−1709.
(28) Gatteschi, D.; Sessoli, R.; Villain, J. *Molecular Nanomagnets;* Oxford University Press: Oxford, U.K., 2006.
(29) Thomas, L.; Lionti, F.; Ballou, R.; Gatteschi, D.; Sessoli, R.; Barbara, B. *Nature* **1996**, *383*, 145−147.
(30) Aubin, S. M. J.; Dilley, N. R.; Pardi, L.; Krzystek, J.; Wemple, M. W.; Brunel, L.-C.; Maple, M. B.; Christou, G.; Hendrickson, D. N. *J. Am. Chem. Soc.* **1998**, *120*, 4991−5004.
(31) Wernsdorfer, W.; Sessoli, R. *Science* **1999**, *284*, 133−135.
(32) Bogani, L.; Wernsdorfer, W. *Nat. Mater.* **2008**, *7*, 179−186.
(33) Cervetti, C.; Heintze, E.; Bogani, L. *Dalton Trans.* **2014**, *43*, 4220−4232.
(34) Thiele, S.; Balestro, F.; Ballou, R.; Klyatskaya, S.; Ruben, M.; Wernsdorfer, W. *Science* **2014**, *344*, 1135−1138.
(35) Urdampilleta, M.; Klyatskaya, S.; Cleuziou, J. P.; Ruben, M.; Wernsdorfer, W. *Nat. Mater.* **2011**, *10*, 502−506.
(36) Cornia, A.; Mannini, M. *Molecular Nanomagnets and Related Phenomena* in the "Structure and Bonding" book series; Springer: Berlin Heidelberg, 2014; pp 1−38.
(37) Ababei, R.; Pichon, C.; Roubeau, O.; Li, Y.-G.; Bréfuel, N.; Buisson, L.; Guionneau, P.; Mathonière, C.; Clérac, R. *J. Am. Chem. Soc.* **2013**, *135*, 14840−14853.
(38) Miyasaka, H.; Nakata, K.; Lecren, L.; Coulon, C.; Nakazawa, Y.; Fujisaki, T.; Sugiura, K.; Yamashita, M.; Clérac, R. *J. Am. Chem. Soc.* **2006**, *128*, 3770−3783.
(39) Miyasaka, H.; Nakata, K.; Sugiura, K.-i.; Yamashita, M.; Clérac, R. *Angew. Chem., Int. Ed.* **2004**, *43*, 707−711.
(40) Batten, S. R.; Champness, N. R.; Chen, X.-M.; Garcia-Martinez, J.; Kitagawa, S.; Ohrstrom, L.; O'Keeffe, M.; Suh, M. P.; Reedijk, J. *CrystEngComm* **2012**, *14*, 3001−3004.
(41) Biradha, K.; Ramanan, A.; Vittal, J. J. *Cryst. Growth Des.* **2009**, *9*, 2969−2970.
(42) Galloway, K. W.; Schmidtmann, M.; Sanchez-Benitez, J.; Kamenev, K. V.; Wernsdorfer, W.; Murrie, M. *Dalton Trans.* **2010**, *39*, 4727−4729.
(43) Chen, M.; Sañudo, E. C.; Jiménez, E.; Fang, S.-M.; Liu, C.-S.; Du, M. *Inorg. Chem.* **2014**, *53*, 6708−6714.
(44) Wei, X.-H.; Yang, L.-Y.; Liao, S.-Y.; Zhang, M.; Tian, J.-L.; Du, P.-Y.; Gu, W.; Liu, X. *Dalton Trans.* **2014**, *43*, 5793−5800.
(45) Woodruff, D. N.; Winpenny, R. E. P.; Layfield, R. A. *Chem. Rev.* **2013**, *113*, 5110−5148.
(46) Feltham, H. L. C.; Brooker, S. *Coord. Chem. Rev.* **2014**, *276*, 1−33.
(47) Sorace, L.; Benelli, C.; Gatteschi, D. *Chem. Soc. Rev.* **2011**, *40*, 3092−3104.
(48) Rinehart, J. D.; Long, J. R. *Chem. Sci.* **2011**, *2*, 2078−2085.
(49) Inose, T.; Tanaka, D.; Tanaka, H.; Ivasenko, O.; Nagata, T.; Ohta, Y.; De Feyter, S.; Ishikawa, N.; Ogawa, T. *Chem.—Eur. J.* **2014**, *20*, 11362−11369.
(50) Lin, P.-H.; Burchell, T. J.; Ungur, L.; Chibotaru, L. F.; Wernsdorfer, W.; Murugesu, M. *Angew. Chem., Int. Ed.* **2009**, *48*, 9489−9492.
(51) Takamatsu, S.; Ishikawa, T.; Koshihara, S. Y.; Ishikawa, N. *Inorg. Chem.* **2007**, *46*, 7250−7252.
(52) Ishikawa, N. *Polyhedron* **2007**, *26*, 2147−2153.
(53) Ishikawa, N.; Sugita, M.; Wernsdorfer, W. *J. Am. Chem. Soc.* **2005**, *127*, 3650−3651.
(54) da Cunha, T. T.; Jung, J.; Boulon, M. E.; Campo, G.; Pointillart, F.; Pereira, C. L. M.; Le Guennic, B.; Cador, O.; Bernot, K.; Pineider, F.; Golhen, S.; Ouahab, L. *J. Am. Chem. Soc.* **2013**, *135*, 16332−16335.
(55) Ganivet, C. R.; Ballesteros, B.; de la Torre, G.; Clemente-Juan, J. M.; Coronado, E.; Torres, T. *Chem.—Eur. J.* **2013**, *19*, 1457−1465.
(56) Baldoví, J. J.; Cardona-Serra, S.; Clemente-Juan, J. M.; Coronado, E.; Gaita-Ariño, A.; Palii, A. *Inorg. Chem.* **2012**, *51*, 12565−12574.
(57) AlDamen, M. A.; Cardona-Serra, S.; Clemente-Juan, J. M.; Coronado, E.; Gaita-Arino, A.; Marti-Gastaldo, C.; Luis, F.; Montero, O. *Inorg. Chem.* **2009**, *48*, 3467−3479.
(58) Boulon, M. E.; Cucinotta, G.; Luzon, J.; Degl'Innocenti, C.; Perfetti, M.; Bernot, K.; Calvez, G.; Caneschi, A.; Sessoli, R. *Angew. Chem., Int. Ed.* **2013**, *52*, 350−354.
(59) Cucinotta, G.; Perfetti, M.; Luzon, J.; Etienne, M.; Car, P.-E.; Caneschi, A.; Calvez, G.; Bernot, K.; Sessoli, R. *Angew. Chem., Int. Ed.* **2012**, *51*, 1606−1610.
(60) Jung, J.; Le Natur, F.; Cador, O.; Pointillart, F.; Calvez, G.; Daiguebonne, C.; Guillou, O.; Guizouarn, T.; Le Guennic, B.; Bernot, K. *Chem. Commun.* **2014**, *50*, 13346−13348.
(61) Yi, X. H.; Bernot, K.; Calvez, G.; Daiguebonne, C.; Guillou, O. *Eur. J. Inorg. Chem.* **2013**, 5879−5885.
(62) Yi, X.; Bernot, K.; Pointillart, F.; Poneti, G.; Calvez, G.; Daiguebonne, C.; Guillou, O.; Sessoli, R. *Chem.—Eur. J.* **2012**, *18*, 11379−11387.
(63) Pinsky, M.; Avnir, D. *Inorg. Chem.* **1998**, *37*, 5575−5582.
(64) Casanova, D.; Cirera, J.; Llunell, M.; Alemany, P.; Avnir, D.; Alvarez, S. *J. Am. Chem. Soc.* **2004**, *126*, 1755−1763.
(65) Cirera, J.; Ruiz, E.; Alvarez, S. *Chem.—Eur. J.* **2006**, *12*, 3162−3167.
(66) Blatov, V. A.; Shevchenko, A. P.; Proserpio, D. M. *Cryst. Growth Des.* **2014**, *14*, 3576−3586.
(67) Guo, Y.-N.; Xu, G.-F.; Guo, Y.; Tang, J. *Dalton Trans.* **2011**, *40*, 9953−9963.
(68) Zhou, H.-C.; Long, J. R.; Yaghi, O. M. *Chem. Rev.* **2012**, *112*, 673−674.
(69) Czaja, A. U.; Trukhan, N.; Muller, U. *Chem. Soc. Rev.* **2009**, *38*, 1284−1293.

DOI: 10.1021/acs.inorgchem.5b00087
Inorg. Chem. 2015, 54, 5213−5219

(70) Roy, S.; Chakraborty, A.; Maji, T. K. *Coord. Chem. Rev.* **2014**, *273*−*274*, 139−164.

DOI: 10.1021/acs.inorgchem.5b00087
Inorg. Chem. 2015, 54, 5213−5219